FULL CRASH TEST RECONSTRUCTION AND ANALYSIS OF FOUR REAL-WORLD IMPACTS

Melanie Franklyn, David Logan, Peter Hillard and Brian Fildes
Monash University Accident Research Centre (MUARC), Victoria, Australia.

ABSTRACT – Reconstruction of real-world crashes using computer software has been performed by previous researchers, as demonstrated by numerous studies in the literature. However, this method has a number of disadvantages, particularly with regard to the accuracy of the crash reconstruction software used to replicate real-world crashes. In the current research, full physical crash test reconstructions of four real-world crashes were conducted. For each case, a comparison of crash test damage between the real-world and crashed vehicles was performed, and injury parameters from the anthropomorphic test devices were evaluated against the actual injuries sustained by the real-world occupants. The results demonstrated that the crash damage profiles produced, despite some variation, were a reasonable replication of the real-world damage, with some over or underestimation of the damage in each case. Injury assessment functions from the anthropomorphic test devices correlated well with the real-world injuries in almost all instances. Hence, despite some degree of over or underestimation of crush in the crash test reconstructions, the results indicate that the acceleration experienced by the anthropomorphic test devices must have been similar to that experienced by the real-world occupants. This suggests that injury parameters measured by anthropomorphic test devices do not entirely depend on vehicle crush, but also on other crash parameters.

INTRODUCTION

The process of developing full simulations of real-world crashes is firmly established as a method for better understanding occupant kinematics and injury mechanisms (eg. Menon et al., 2003; Geigl et al., 2003). These studies typically utilise data collected from an actual crash such as vehicle damage and crash severity estimates, coupled with vehicle paths and resting positions from both vehicle occupants and police reports. This data is used to generate a computer simulation of the crash in a program such as HVE or PC-CRASH, the output of which can then be used as the input to a MADYMO simulation model thus allowing the movement and loading of anthropomorphic test devices (ATD's) to be examined. However, this technique has a number of limitations. Real-world dynamics during a crash, in terms of both vehicle movement and structural behaviour, are invariably more complex than can be replicated by most available computer reconstruction programs. As a result, the kinematics of the MADYMO occupant ATD models are limited by the input data from the reconstruction programs.

This study is one of the first to address these limitations by recreating the real-world crash in a controlled environment. Instrumented vehicles and dummies permit accurate verification of the occupant kinematics and, most importantly, the loading levels experienced by the ATD which can then be directly correlated with the injuries sustained by the real-world crash occupants.

METHODS

This study is comprised of two separate components: Crash Investigation and Crash Reconstruction.

Crash Investigation

The Monash University Accident Research Centre (MUARC) Crash Investigation Team collects data on real-world crashes in Victoria, New South Wales (NSW), and Tasmania, Australia, with approximately 55% of cases being collected in urban areas. The team is comprised of Vehicle Inspectors, Research Nurses, Crash Site Investigators, a crash investigation researcher specialising in Ethics, and a Senior Manager. The case occupants are recruited by a Research Nurse, as the Crash Investigation Team use a hospital-based inclusion criterion, which means that at least one of the occupants in the crash must have been hospitalised. After a patient is recruited, the information described below is collected.

Medical Data Collection: A MUARC Research Nurse interviews the patient about a range of factors pertaining to the collision, such as the crash scenario, their seating position in the vehicle etc. The medical information pertaining to the crash is then recorded and the injuries are subsequently coded according to the Abbreviated Injury Scale (AIS) 1990 (Revision 1998). CT reports, other diagnostic imaging reports and medical reports are accessed in order to accurately describe and code the injuries.

Vehicle Inspection: The patient's vehicle is located and a vehicle inspection is performed typically within days of the crash in accordance with international best practice for retrospective examination of crash-damaged vehicles (NHTSA, 1989). The inspection includes details about the vehicle itself (such as make, model, year, VIN and measurements of the vehicle body and wheelbase) in addition to collision-specific data (such as crush dimensions and seatbelt use). The crush dimensions are recorded according to SAE J224 Collision Deformation Classification (CDC) profile and the delta-V is computed using CRASH3. The Principal Direction of Force (PDoF) is visually determined both directly from the vehicle and based on an understanding of the pre-collision vehicle(s) paths.

Crash Site Inspection: Information from the patient and tow truck operators are used in conjunction with police reports to locate the crash site and sketch the crash scenario. Various angles of the crash site are photographed and evidence of the crash, such as broken glass or paint marks on the struck object, are identified. If the vehicle impacted into a fixed object, such as a tree or pole, measurements of the object are also recorded. If there is more than one vehicle involved in the crash, the collision partner is located where possible, and an inspection of the second vehicle is also performed. After all data has been collected, a summary sheet describing the key aspects of the crash is produced. Lastly, members of the Crash Investigation Team take part in a case review panel, where any complex or inconsistent case details are discussed and resolved. Lastly, all information is de-identified and the case entered into a database and filed.

Four cases involving a specific model of a large Australian sedan were selected for this study. These cases were selected to firstly provide a range of different impact types, and secondly, on the basis that they were not too complex to be reliably replicated via crash tests. Selection criteria included cases which could be reconstructed with a crash test speed below 90km/hr and cases where there were only adult occupants in the vehicle. Crashes where the occupants were unbelted or believed to be out of position were excluded.

Crash Reconstruction

Computer Simulations: Before conducting any physical crash tests, computer simulations of the crashes were performed in order to determine approximate values of pre-crash speeds and if relevant, crab angles. Using a combination of the simulations and advice from technical experts,

the final crash test speed was then decided. Two types of simulations were performed. The first set of simulations used one of two SMAC (Simulation Model of Automobile Collisions) based programs, either the SMAC4 module of the HVE (Human Vehicle Environment) software (Version 4.30, EDC, OR, US), or PC-Crash (Version 6.2, MacInnis Engineering Associates), simulations were performed until parameters such as the crash scenario, CDC profile from the vehicle inspection and the delta-V matched those derived from the real-world crash. Neither HVE or PC-Crash had the exact model vehicles in their databases, hence vehicles similar to the real-world vehicles were used and modified so that parameters such as the drive axle location, vehicle weight, number of doors and type of vehicle (e.g. sedan) closely matched the vehicles required for the analysis. The crash test facility could only accommodate one moving vehicle. Consequently, if there were two moving vehicles in the real-world case, further simulations were performed to find the speed required to perform the crash test with a stationary target vehicle. The second set of simulations was performed using a Finite Element (FE) model of the case vehicle, and if applicable, an FE model of the non-case vehicle. The initial contact point and the impact speed were varied throughout several iterations until the model-calculated deformation patterns were similar to those measured in the real-world impact.

Crash Test Reconstruction: Vehicles of the same model and year as the case vehicles were acquired and prepared for the crash tests. Detailed information relating to the vehicle preparation is presented in the Results section. Standard injury metrics were measured and the data were filtered according to SAE J211 specifications and then compared to the recommended Injury Assessment Reference Value's (IARV's) in order to assess injury potential for various body regions.

RESULTS

Crash Investigation

A summary of the four cases selected for this study is provided below. Pictures of real-world and crash test vehicles have been cropped so that vehicles cannot be identified, while allowing the damage to be viewed. The real-world vehicles are shown in Figure 1.

Case 1

A 1993 small coupè (bullet vehicle) struck a large passenger sedan (target vehicle) on the driver's side (right) after running a red light. The target vehicle rotated almost 180 degrees clockwise and then impacted a pole at the front of the vehicle on the passenger's side (left). The secondary pole impact was not reconstructed because the injuries to the occupants in the target vehicle were attributed to the primary impact. There were two occupants seated in the target vehicle: a male driver (the case occupant) and a female front seat passenger (FSP). The male occupant was 56 years old, 1.79m and 80kg while the female occupant was 51 years old, 1.59m and 65kg. Both occupants were wearing seatbelts. Frontal and side airbags were fitted to the vehicle and both airbags deployed in the crash. The only occupant of the bullet vehicle was the driver, who was female. Medical details pertaining to the driver of the bullet vehicle were not collected as she was not recruited into the study. Figures 1a to 1c show the real-world vehicles.

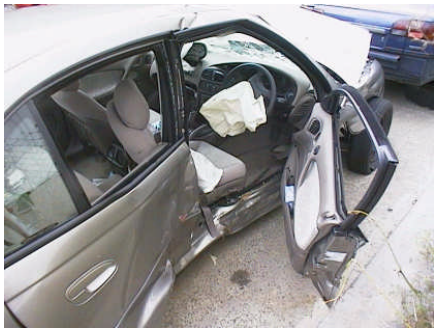

(a) Case 1: Target vehicle showing the lateral impact.

(b) Case 1: Target vehicle showing pole impact.

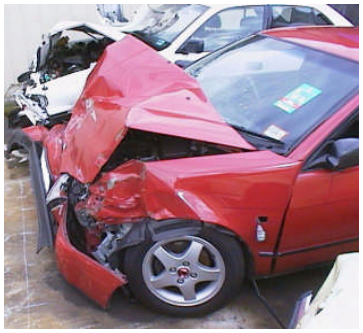

(c) Case 1: Bullet vehicle.

(d) Case 2: Target vehicle.

(e) Case 2: The impacted tree.

(f) Case 3: Target vehicle.

(g) Case 3: The impacted pole.

(h) Case 4: Target vehicle.

(i) Case 4: Base of the road sign pole.

Figure 1. Real-world crashed vehicles and collision partners.

Case 2

The driver of a large passenger sedan lost control of his vehicle on a bend in the road and hit a tree on the passenger's side (left). The vehicle is shown in Figure 1d while the tree is shown in Figure 1e. The only occupant of the vehicle was the driver, who was 46 years old, 178cm in height and weighed 95kg. He was wearing a seatbelt at the time of the crash. Three airbags were

fitted, a steering wheel airbag and two seat-mounted side impact airbags, but only the passenger seat mounted airbag deployed during the crash.

Case 3

The driver of a large passenger sedan lost control of his vehicle and clipped a parked vehicle on the front passenger side (left). He then struck a telegraph pole on the driver's side (right), which resulted in extensive cabin intrusion. Only the second collision was reconstructed as the injuries sustained were attributed to the impact with the pole. There were two occupants in the vehicle, a driver and a FSP. The driver, who was the case occupant, was a 39-year-old male who was 180cm in height and weighed 80kg. The FSP was a male of similar anthropometric dimensions to the driver. Both occupants were belted. The FSP was admitted to a non-study hospital, hence his injuries could not be recorded. Figure 1f shows the real-world vehicle, and Figure 1g the pole.

Case 4

The driver of a large passenger sedan lost control of his vehicle while travelling on a freeway and subsequently hit a road sign pole on the side of the freeway. The driver, an 18-year-old male, was the sole occupant. He was 190cm tall and weighed 73kg, and was belted at the time of the crash. The real-world vehicle is shown in Figure 1h, while Figure 1i demonstrates the road sign pole.

Crash Reconstruction

Crash Test Reconstructions

This section describes how the physical crash test reconstructions were conducted for each case, and presents the results from the crash tests. Crash configurations are demonstrated in Figure 2, while Figure 3 shows the crashed vehicles. The raw injury data was filtered using Diadem Versions 7.2 (Case 3) and 8.0 (Cases 1, 2 and 4). Different versions were used as the software was updated during the study. The percentage IARV (%IARV) was calculated by dividing the experimentally measured injury prediction value by the regulation injury threshold (the IARV), then multiplying by 100. A %IARV greater than 100 indicates that the injury matrix measured has exceeded the recommended injury threshold. The %IARV's from the ATDs were compared to the real-world injuries in order to assess the accuracy of the reconstruction.

Case 1

The required pre-impact crash test speed was computed to be 85km/hr, but as the winch was manually operated, the final crash test speed attained was 85.74km/hr. The pre-calculated crab angles needed were 43 degrees for the target vehicle and 47 degrees for the bullet vehicle – this double crab configuration was used as the crab angle was too large to replicate at the test facility. In order to generate the crab angle, the bullet vehicle was mounted onto a trolley. To compensate for the trolley mass of 200kg, an equivalent mass of vehicle components were removed from the bullet vehicle such that the position of the centre of gravity was not altered. Both on and off-board cameras recorded the motion of the vehicle and the ATD's. The crash test configuration is shown in Figure 2a. To represent the two occupants in the target vehicle, the ATD's used were a 50th percentile BioSID for the driver and a SIDIIs for the FSP. There were 50 data channels for the BioSID, while the SIDIIs had 26 channels. The Hybrid III in the bullet vehicle was not instrumented as the injuries to the real-world occupant of the bullet vehicle had not been documented. A total of 9 contact switches was installed and airbag and pretensioner fire times were recorded. In total, 101 channels were used for the crash reconstruction. Figures 3a and 3b show the damage to the crash test vehicles.

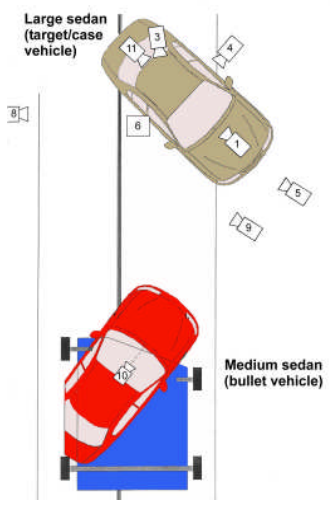

(a) Crash test configuration for Case 1.

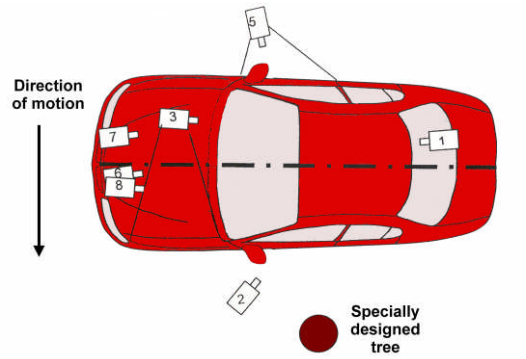

(b) Crash test configuration for Case 2. Case Cameras 1-3 and 5-8 are shown, while camera 4 was an off-board overhead camera and is not shown in the diagram.

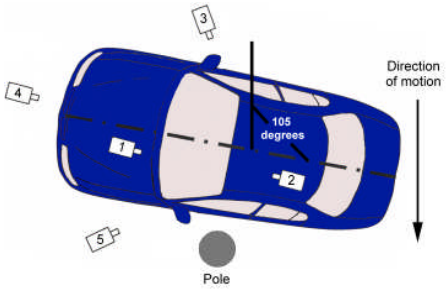

(c) Crash test configuration for Case 3. Cameras 2 and 6 were off-board and hence are not illustrated.

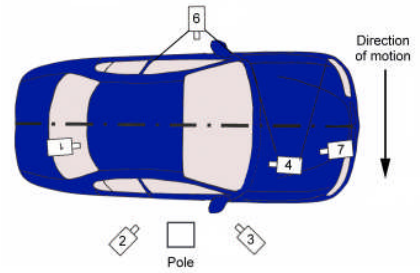

(d) Crash test configuration for Case 4. Camera 5 was an overhead camera and is not illustrated.

Figure 2. Crash test configurations for each of the real-world crash test reconstructions.

Case 2

The final crash test speed was 61.02km/hr, and no crab angle was used (Figure 2b). The reconstruction involved towing the vehicle into a specially designed pole (Figure 3d), which was angled to represent both the angle of the tree and the angle the vehicle adopted at the final rest position due to the topography of the ground. A 50th percentile BioSID ATD was used to represent the driver. There were 54 data channels attached to the ATD, two contact switches were instrumented and airbag and pretensioner fire times were recorded, making a total of 62 channels. Figure 3c demonstrates the damage to crash test vehicle.

Case 3

The vehicle was towed laterally into a fixed pole (Figure 3f) at a speed of 43km/hr. The pole was of fixed diameter and was welded to the ground so it was perpendicular to the ground. The vehicle available was a left-hand drive, hence a mirror image crash test was conducted so that the crash remained a near-side impact. A small crab angle was used to simulate the 255 degree PDoF (Figure 2c). The driver ATD used was a 50th percentile BioSID. The FSP was a 50th percentile SID (a second BioSID was unavailable at the time), but as the driver was the case occupant, any 50th percentile ATD was sufficient to represent the FSP. The BioSID was instrumented with 50 data channels. There were 7 cameras installed to record the motion of the vehicle and its

occupants and 5 contact switches were used. Airbag and pretensioner fire times were recorded. A total of 57 channels was used for the entire crash test. The post-test damage can be observed in Figure 3e.

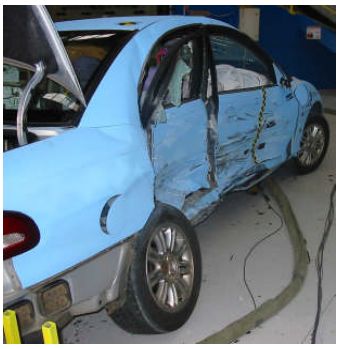

(a) Case 1: Target vehicle showing the lateral impact

(b) Case 1: Bullet vehicle

(c) Case 2: Target vehicle

(d) Case 2: Pole used to replicate tree.

(e) Case 3: Target vehicle.

(f) Case 3: Target vehicle showing impacted pole.

(g) Case 4: Target vehicle.

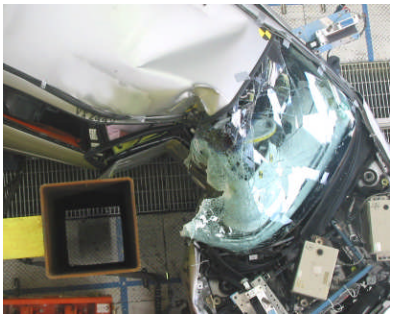

(h) Case 4: Pole with post-crashed vehicle.

Figure 3. Post crash test damage to the vehicles and collision partners.

Case 4

The final crash test speed chosen was 58km/hr and no crab angle was used (Figure 2d). As the pole was an unusual shape (Figure 1h), an identical pole was obtained through the subcontractor who assembled the original poles. A 50th percentile BioSID ATD was used to represent the driver. There were 56 data channels attached to the ATD, and airbag and pretensioner fire times were recorded. The vehicle damage is shown in Figure 1g.

Crash Test Data

Vehicle inspection measurements from the real-world crash against the dimensions measured after the physical crash test are displayed in Table 1. Each of the cases is considered below.

Case 1

The CDC for the real-world and crash test target vehicles were identical, indicating that the damage produced in the crash test was a reasonable outcome. A comparison of damage measures (e.g. maximum crush depth and Energy) indicates that, for the target vehicle, the crash test damage slightly underestimated the real-world crash damage. The damage profile from the crash test was slightly wider and the maximum crush was further towards the rear of the vehicle compared to the real-world impact (when comparing C3 and C4). A similar analysis of the bullet vehicle shows that the damage produced in the crash test was somewhat greater than in the real-world case, but the accuracy of the damage profile for the bullet vehicle was not as important as that of the target vehicle. Overall, the crash test appeared to be a reasonable representation of the real-world crash.

Case 2

The C1-C6 measurements show that the maximum amount of lateral intrusion in the crash test (135cm) was slightly more than the maximum amount of lateral intrusion resulting from the real-world crash (101cm). The resulting BEV and energy values produced from the crash test vehicle were also greater than in the real-world crash. This was due to both the maximum lateral intrusion and the direct damage width being greater in the crash test vehicle than in the real-world case vehicle. In summary, the crash appeared to be a reasonable representation of the real-world crash.

Case 3

A comparison of the CDC values from both the real-world case (03RPAW5 right-hand drive) and the reconstructed case (09LPAW4 left hand drive) indicates that the deformation profile was similar. Although the CDC profile produced was alike, the crash test damage somewhat underestimated the real-world crash damage, which was evident when comparing parameters such as the BEV, the Energy, the direct damage width and the C1-C6 measurements.

Case 4

A comparison of the results shows that the crash test appears to be a good representation of the real-world crash, as the BEV and Energy were close in both cases. The maximum intrusion was greater in the crash test vehicle than the real-world vehicle, but the BEV was slightly greater in the real-world vehicle as the damage spanned a greater length of the vehicle.

Injury Data

The injuries to the real-world occupants in each case are shown in Table 2, while Figure 4 presents a graphical representation of the %IARV's to the ATD's.

Table 1. Comparison of vehicle measurements between the real-world crash and the crash test for all cases.

	Case 1				Case 2		Case 3		Case 4	
Parameter	**Real-world target vehicle**	**Crash test target vehicle**	**Real-world bullet vehicle**	**Crash test bullet vehicle**	**Real-world**	**Crash test**	**Real-world**	**Crash test**	**Real-world**	**Crash test**
C1	0 cm	5 cm	**63 cm**	**103.5 cm**	0 cm	0 cm	0 cm	5 cm	0 cm	0 cm
C2	19 cm	15 cm	41 cm	74 cm	58 cm	13 cm	40 cm	13 cm	7 cm	21 cm
C3	**33 cm**	20 cm	32 cm	64 cm	**101 cm**	39 cm	**95 cm**	38 cm	63 cm	61 cm
C4	31 cm	**23 cm**	33 cm	68 cm	64 cm	**135 cm**	49 cm	**64 cm**	**82 cm**	**91 cm**
C5	25 cm	20 cm	34 cm	78 cm	15 cm	26 cm	20 cm	32 cm	61 cm	53 cm
C6	0 cm	5 cm	45 cm	79 cm	0 cm	0 cm	0 cm	5 cm	0 cm	0 cm
Maximum crush depth	**33 cm**	**23 cm**	**63 cm**	**104 cm**	**101 cm**	**135 cm**	**95 cm**	**64 cm**	**82 cm**	**91 cm**
Direct damage width	177 cm	190 cm	166 cm	165 cm	50 cm	80 cm	55 cm	40 cm	49 cm	65 cm
Length of vehicle offside	428 cm	485 cm	324 cm	335 cm	467 cm	443 cm	412 cm	455 cm	465 cm	402 cm
Length of vehicle nearside	464 cm	474 cm	347 cm	#	453 cm	343 cm	450 cm	405 cm	480 cm	442 cm
Width of vehicle	176 cm	180 cm	166 cm	165 cm	184 cm	184.2 cm	150 cm	180 cm	184 cm	182.2 cm
CDC	**03RPEW3**	**03RPEW3**	**12FDEW3**	**12FDEW4**	**09LYAW5**	**09LPAW5**	**03RPAW5**	**09LPAW4**	**03RPAW4**	**03RPAW4**
Distance rear to C1	190 cm	75 cm	0 cm	0 cm	112 cm	130 cm	130 cm	130 cm	132 cm	162 cm
Distance front to C6	90 cm	150 cm	0 cm	0 cm	135 cm	113 cm	65 cm	140 cm	112 cm	84 cm
Distance C1 to C6	240 cm	260 cm	166 cm	165 cm	198 cm	120 cm	200 cm	185 cm	185 cm	171 cm
Offset	+35 cm	+39.6 cm	0 cm	0 cm	+34 cm	-96 cm	+79.6 cm	+22.1 cm	+56 cm	+58 cm
Delta-V	**26 km/hr**	**35 km/hr**	**45 km/hr**	**68 km/hr**	**50 cm**	**61 km/hr**	**39 km/hr**	**31 km/hr**	**41 km/hr**	**38 km/hr**
Energy	**45 kJ**	**34 kJ**	**80 kJ**	**24 kJ**	**159 kJ**	**248 kJ**	**132 kJ**	**67 kJ**	**1227 kJ**	**1203 kJ**

Table 2. Injuries to the real-world occupants.

Case	Body region	Injury	AIS	Case	Body Region	Injury	AIS
1	Head	None	0	3	Facial, neck, shoulder	None	0
	Face, neck, shoulder	None	0		Chest and abdominal	Flail chest (fracture of 4th, 5th and 6th ribs)	3
	Chest and abdominal	5 R rib fractures and haemopneumothorax	4			Haemopneumothorax (L and R)	3
	Pelvis	Contusion to R hip	1		Pelvis	Fractures of the R inferior and superior pubic rami	2
	Lower limbs	Multiple abrasions to L femur	1		Lower limbs	Fractured L femur (comminuted transverse)	3
2	Head	Fracture to petrous pyramid with GCS=11 at scene	4	4	Head	R inferior frontal lobe EDH (14mm)	5
	Face, neck, shoulder	Multiple grazes to face; L and R shoulder bruising	1, 1			R anterior temporal lobe SDH (9mm)	4
	Chest and abdominal	Bibasal areas of lung contusion	4			Cerebral swelling; partial effacement of some basal cisterns	4
		Mild T7 crush with 10-15% loss of height, canal intact	2			R inferior cortical contusions with 5mm midline shift to L	3
		Spiral fracture neck of 1st rib posteriorly	1			Comminuted fracture R orbital roof	3
		Renal contusion with small subcapsular haematoma	2			R optic neuropathy and cranial nerve palsy	2, 2
		Lower abdominal bruising	1			Pneumocephalus (not codeable as other head injuries)	N/A
	Pelvis/Lower limbs	None	0			Multiple AIS 2 and AIS 1 facial injuries	1, 2
	External	Multiple lacerations and abrasions	1		Chest	Contusions to L and R lower lung zones	4
3	Head	Bilateral extradural haematoma (temporal)	5		Pelvis	Superior L pubic ramus fractures	2
		Temporal lobe contusion and GCS=3 at scene	3			Inferior L pubic ramus fracture	2
		Bilateral temporal bone fracture	3			Fracture of R sacral ala	2
		Bilateral sphenoid bone fracture	3		Lower limbs	Closed transverse fracture midshaft R femur	3

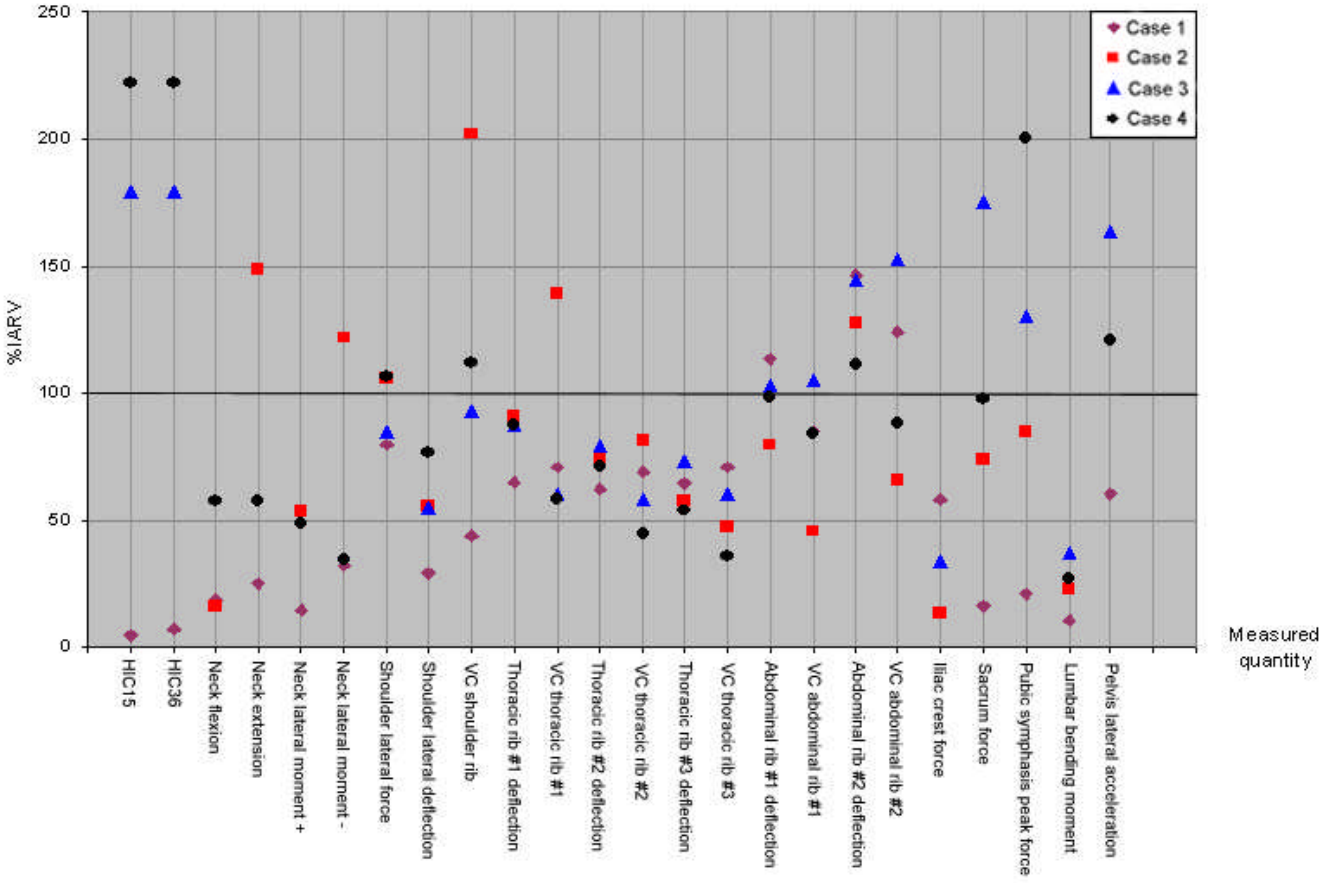

Figure 4: ATD injury responses for each of the cases in the study.

Recalling that a %IARV over 100 indicates that the injury matrix measured has exceeded the recommended injury threshold, values around 100 suggest that the occupant would have sustained a mild injury to that body region. Values considerably over 100 indicate that the occupant would sustain a severe injury to the body region, while values well below 100 suggest that the occupant would sustain no injury, or a very mild injury, to that body region. Comparison of these measures demonstrates how well the ATD represents the real-world occupant. Each of these cases is reviewed below.

Case 1

A review of the data measured from the ATD shows that the abdominal ribs were the only body region to show %IARV's moderately to well over 100, with both deflection, which is used to assess bone injury, and the Viscous Criterion (VC), which is used to assess soft tissue injury, affected. This was consistent with the injuries to the real-world case occupant, who sustained rib fractures and haemopneumothorax. The %IARV's indicated that there would be no (or very mild) head, neck or pelvic injuries to the occupant, which was in agreement with the real-world occupant, who only sustained abrasions in addition to a contusion to the lower limbs, and no head or neck injuries.

Case 2

The HIC (Head Injury Criterion) could not be evaluated using the Diadem software in this case, as one of the ATD head leads detached during the crash test. The %IARV's in some of the ribs were moderate to high. In particular, the VC criteria for thoracic rib#1 and the deflection of abdominal rib#2 were well over the injury threshold, suggesting both bony and soft tissue

injuries to the occupant. This finding was in agreement with the real-world occupant, who sustained thoracic and abdominal injuries. The VC for the shoulder rib indicated that shoulder injuries might be expected in the real-world occupant, but this was not the case. This is considered further in the Discussion section.

Case 3

According to the %IARV's, the occupant would be expected to sustain a reasonably severe head injuries in conjunction with pelvic injuries, both of which were consistent with the real-world occupant who sustained a number of moderate to severe head injuries (skull fractures, a temporal lobe contusion and an extradural haematoma) along with pelvic fractures. The %IARV's also indicate that the occupant would sustain both bony (as measured by rib deflection) and soft tissue (as measured by VC) chest injuries, as the abdominal rib %IARV's were moderate to high. The real-world occupant sustained both rib fractures in addition to haemopneumothorax, hence the injury functions measured from the ATD are in agreement with the severity of injury sustained by the real-world occupant.

Case 4

The %IARV's indicate that the occupant would be expected to sustain severe head injuries, which was in agreement with the real-world occupant who sustained a number of severe head injuries ranging in severity from AIS 2 to AIS 5. Other injuries expected would be to the pubic region and abdominal region. The real-world occupant sustained a number of pubic rami fractures and contusions to the lower lung, hence these findings appear to be in agreement with the real-world injuries. According to the %IARV's, some shoulder injuries might be expected but not seen in the real-world occupant. This is discussed further below.

DISCUSSION

In this research, the use of real-world crashes enabled the biofidelity of the model predictions to be calibrated since actual patient injuries rather than injury criteria were compared with model predictions. Nevertheless, it is difficult to perform a physical crash test that replicates a real-world crash precisely, as crash test precision is limited by how well aspects of the specific real-world crash are understood. In the current study, information about the crashes was collected from various reliable sources and checked against the evidence from the vehicles and crash site for accuracy. Computer simulations were also performed prior to the crash test in order to determine approximate speeds and crab angles required, but as mentioned previously, computer reconstruction programs have a number of limitations. Consequently, reasonably accurate crash tests could be performed within the constraints of the equipment available, as each real-world crash had its own unique characteristics which had to be replicated for the crash test.

The crush profiles for each of the cases in this study were reasonably similar to the crush from the real-world cases. However, there was some under or overestimation in each case, as parameters such as exact speed prior to the impact and the precise angle the impact occurred at are difficult to determine. Nevertheless, in all cases, the values of the injury assessment functions measured from the ATD predicted the severity of the real-world injuries in most body regions for all cases. The only exception appeared to be for the shoulder where the %IARV's appeared to be slightly higher than expected when compared to the injuries to the real-world occupants. However, the shoulder in particular is probably a less critical body region in terms of injury, and

shoulder injury thresholds have received less attention in the literature. Consequently, the results of the current study suggested that injury functions could be accurately determined despite some over or underestimation in crash damage, which suggests that ATD kinematics is not contingent on vehicle crush, but that it also depends on other crash parameters.

In future research, a number of other world crashes will be fully reconstructed in order to have a larger complement of cases in which to perform the following stage of this study. This phase will be to find the other crash parameters which contribute to ATD kinematics, then subsequently develop an algorithm which will incorporate the relative contribution of each of these parameters.

CONCLUSION

This study presents the data for four full physical crash test reconstructions of real-world cases. In each case, the crash damage was similar to the damage to the real-world vehicle, but with some degree of under or overestimation in each case. However, an evaluation of the data from the ATD's revealed that in nearly all body regions for all cases, the %IARV correlated with the severity of injury sustained by the real-world occupant. Hence the results of this study indicate that, ATD response depends only partially on vehicle crash, and consequently must also partially depend on other crash-based parameters. Thus, crash damage is not the only parameter to consider when assessing the accuracy of crash.

ACKNOWLEDEMENTS

The authors would like to acknowledge Ron Laemmle and Ted Olsson for vehicle inspections, to David Kenny for useful discussions on the real-world crashes and the MUARC Crash Investigation Team. Thanks also to Stu Smith, Jacek Wawrzynczak, Dean Niclasen, James MacIntosh and Mark Forbes (Holden) for their involvement in the planning and crash tests.

REFERENCES

Abbreviated Injury Scale (AIS) 1990 Revision, Update 98. Association for the Advancement of Automotive Medicine (1998).

Geigl B.C., Hoschopf H., Steffan H. and Moser A (2003). Reconstruction of occupant kinematics and kinetics for real world accidents. International Journal of Crashworthiness. Vol 8 (1), pp. 17-27.

Menon R.A., Ghati, Y.S., Marigowda, S.B., Arbogast, K.B. and Winston, F.K. (2003). Reconstruction of real world side impact vehicle collisions using HVE – a case series of pediatric pelvic fracture. HVE Forum, 2003.

NHTSA (1989). National Accident Sampling System 1989 Crashworthiness Data System (NASS CDS). Washington DC, US.